A 5-GHz SOUTHERN HEMISPHERE VLBI SURVEY OF COMPACT RADIO SOURCES. I.

Z.-Q. Shen

Harvard-Smithsonian CfA, 60 Garden Street, Cambridge, Massachusetts 02138
and Shanghai Astronomical Observatory, 80 Nandan Road, Shanghai 200030, People's Republic of China

T.-S. Wan

Shanghai Astronomical Observatory, 80 Nandan Road, Shanghai 200030, People's Republic of China

J. M. Moran

Harvard-Smithsonian CfA, 60 Garden Street, Cambridge, Massachusetts 02138

D. L. Jauncey, J. E. Reynolds, A. K. Tzioumis, R. G. Gough, R. H. Ferris, and M. W. Sinclair

Australia Telescope National Facility, CSIRO, Epping, NSW 2121, Australia

D.-R. Jiang, X.-Y. Hong, and S.-G. Liang

Shanghai Astronomical Observatory, 80 Nandan Road, Shanghai 200030, People's Republic of China

M. E. Costa

Department of Physics, University of Western Australia, Nedlands, WA 6009, Australia

S. J. Tingay

Mount Stromlo and Siding Spring Observatories, ACT 2611, Australia

P. M. McCulloch, J. E. J. Lovell, and E. A. King

Department of Physics, University of Tasmania, Hobart, Tasmania 7001, Australia

G. D. Nicolson

Hartebeesthoek Radio Astronomy Observatory, Krugersdorp 1740, South Africa

D. W. Murphy, D. L. Meier, and T. D. van Ommen

Jet Propulsion Laboratory, California Institute of Technology, Pasadena, California 91109

P. G. Edwards[1]

Department of Physics, University of Adelaide, Adelaide, SA 5005, Australia

G. L. White

Department of Physics, University of Western Sydney, Nepean, NSW 2747, Australia
Received 1997 January 15; revised 1997 August 18; accepted 1997 August 18

ABSTRACT

We report the results of a 5-GHz southern hemisphere VLBI survey of compact extragalactic radio sources. These observations were undertaken with the SHEVE array plus Shanghai station in 1992 November. A sample of 22 sources was observed and images of 20 of them were obtained. Of the 20 sources imaged, 15 showed core-jet structure, 1 had a two-sided jet, and 4 had only single compact cores. Eleven of the 16 core-jet (including one two-sided jet) sources showed some evidence of bent jets. No compact doubles were found. A comparison with previous images and the temporal variability of the radio flux density showed evidence for superluminal motion in four of the sources. Five sources were high-energy (>100 MeV) γ-ray sources. Statistical analysis showed the dominance of highly polarized quasars among the detected γ-ray sources, which emphasizes the importance of beaming effect in the γ-ray emission. © *1997 American Astronomical Society.* [S0004-6256(97)04011-9]

[1]Present address: The Institute of Space and Astronautical Science, Sagamihara, Kanagawa 229, Japan.

1. INTRODUCTION

While considerable VLBI imaging and monitoring of extragalactic radio sources have been carried out in the northern hemisphere, the only VLBI surveys undertaken in the south have been the systematic one-baseline intercontinental surveys at 2.3 GHz (Preston *et al.* 1985) and 8.4 GHz (Morabito *et al.* 1986) and the 2.3 GHz imaging and model-fitting SHEVE (Southern Hemisphere VLBI Experiment) survey of 29 sources in 1982 (Preston *et al.* 1989; Meier *et al.* 1989; Tzioumis *et al.* 1989; Jauncey *et al.* 1989, 1994).

In the north, Pearson & Readhead (1981, 1988) conducted a pioneering systematic VLBI survey that produced images of 37 strong extragalactic sources from a complete sample of 65 sources. Most recently, the first Caltech-Jodrell Bank VLBI Survey (CJ1) (Polatidis *et al.* 1995; Thakkar *et al.* 1995; Xu *et al.* 1995) and the second Caltech-Jodrell Bank VLBI Survey (CJ2) (Taylor *et al.* 1994; Henstock *et al.* 1995) imaged 135 and 193 sources, respectively. These programs have produced a systematic classification scheme for compact extragalactic radio sources.

The launch of the Space VLBI missions VSOP (Hirosawa 1991) in 1997 and the intended launch of RadioAstron (Kardashev & Slysh 1988) will lead to a significant increase in resolution over that possible with ground-based radio telescopes alone. In order to make full use of the resources of Space VLBI, preliminary ground-based surveys on intercontinental baselines are essential to identify suitable targets.

With these imperatives to improve the understanding of compact radio sources in the south, we have been conducting a 5-GHz southern hemisphere VLBI radio source survey, with the major aims of: (1) filling the gap in southern VLBI observations; (2) presenting a pre-launch survey for those potential targets for space VLBI; (3) providing first-epoch observations in a search for southern superluminal sources; and (4) identifying compact sources as potential southern calibration and astrometric reference sources. We have undertaken two observing sessions. The first, described here, was completed in 1992 November with the observation of 22 sources. The second was undertaken in 1993 May, when a further 23 sources were observed.

This paper describes the astrophysical results of the first period of observations. We introduce the survey sample (Sec. 2); describe the observations and data reduction procedures (Sec. 3); present the results with emphasis on the 20 sources imaged (Sec. 4); analyze VLBI measurements in light of the detection of active galatical nuclei by EGRET (Energetic Gamma-Ray Experiment Telescope) on the CGRO (Compton Gamma-Ray Observatory) (Sec. 5); and summarize our conclusions (Sec. 6).

2. THE SAMPLE

We selected those southern radio sources with the strongest correlated flux densities at frequencies near 5 GHz to help ensure successful imaging surveys. These extragalactic sources were chosen from the one-baseline intercontinental surveys at frequencies of 2.3 and 8.4 GHz (Morabito *et al.*

1986, and references therein) using the following selection criteria:

(1) Declination: $-45° < \delta < +10°$,
(2) correlated flux densities at 2.3 and 8.4 GHz: $S^c_{2.3 \text{ GHz}} > 0.6$ Jy and $S^c_{8.4 \text{ GHz}} > 0.6$ Jy,
(3) total flux density at 5 GHz: $S^t_{5 \text{ GHz}} > 1.0$ Jy.

Thirty-six sources meet these criteria, including the extensively observed and well-studied sources 3C 273 and 3C 279. These sources are, in order of their right ascensions: 0048−097, 0104−408, 0106+013, 0332−403, 0420−014, 0426−380, 0438−436, 0458−020, 0521−365, 0727−115, 0736+017, 1034−293, 1055+018, 1104−445, 1144−379, 1226+023, 1253−055, 1334−127, 1354−152, 1504−166, 1510−089, 1519−273, 1548+056, 1730−130, 1741−038, 1749+096, 1921−293, 2121+053, 2131−021, 2134+004, 2145+067, 2216−038, 2223−052, 2243−123, 2318+049, and 2345−167. This sample is a subset of the primary list proposed by the Science Objectives Committee for observation by RadioAstron, which has a major selection criterion of correlated flux densities in excess of 0.5 Jy at 2.3 or 8.4 GHz. We chose 20 of the 36 sources for the first experiment, due to the limited observing time available. In addition, we also added two other interesting sources, 0235+164 (well-studied, and a member of the RadioAstron list, but outside the declination range of the criteria) and 1814−637 (strong, but also outside the declination range). All 22 sources could be treated as Parkes sources. They have been optically identified, and redshifts are available for 20 of them. Their names, positions, redshifts, optical types, flux densities, and related information are listed in Table 1.

Of the remaining 16 sources conforming to the above selection criteria, 7 (0332−403, 0426−380, 0438−436, 0521−365, 1034−293, 1226+023 and 2243−123) were observed in 1993 May. The other 9 sources (0727−115, 0736+017, 1055+018, 1253−055, 1354−152, 1749 +096, 2121+053, 2131−021, and 2318+049) will be observed in future experiments. The results of these experiments will be reported later.

3. OBSERVATIONS AND DATA REDUCTION

We performed the survey with the SHEVE network, augmented by the Shanghai station, on 1992 November 20–22. The participating stations were located in Hartebeesthoek (South Africa), Hobart (Australia), Mopra (Australia), Narrabri (Australia), Perth (Australia), and Seshan (Shanghai, China). The station parameters are listed in Table 2. Most of the 22 radio sources in Table 1 were observed in a snapshot mode, i.e., two to five 30-minute scans were obtained. Figure 1 shows a typical (u,v) plot for 1730−130 with three scans in the observations. At the beginning and/or the end of each scan, system temperature measurements for the amplitude calibration were made and the antenna pointing was checked. All data were recorded in VLBI Mark II format with 2-MHz bandwidth and left-circular polarization (IEEE convention) at each station during the observation, and subsequently cross-correlated on the JPL/Caltech Mark II processor in Pasadena, California, in 1994 September.

TABLE 1. Sources observed in 1992 November.

IAU Name (1)	Other (2)	R.A. (3)	Dec. (4)	z (5)	ID (6)	$S^t_{5\,\text{GHz}}$ (7)	Notes (8)
0048−097	OB−080	00 48 09.9773	−09 45 24.336	>0.2	BLO	1.33	1,2,3,5,6,7
0104−408		01 04 27.5777	−40 50 21.697	0.584	BLO?	2.64	1,2
0106+013	4C01.02	01 06 04.5200	+01 19 01.100	2.107	HPQ	2.39	1,2,5,6,7
0235+164	OD160	02 35 52.6341	+16 24 03.920	0.940	BLO	4.26	1,2,5,6,7
0420−014	OA129	04 20 43.5424	−01 27 28.735	0.915	HPQ	4.01	1,2,3,5,6,7
0458−020	4C−02.19	04 58 41.2800	−02 03 34.500	2.286	HPQ	3.23	1,2,5,6,7
1104−445		11 04 50.3766	−44 32 52.879	1.598	WPQ	3.07	1,2
1144−379		11 44 30.8624	−37 55 30.531	1.048	BLO	4.60	1,2,7
1334−127	OP−158.3	13 34 59.8036	−12 42 09.633	0.541	HPQ	5.08	1,2,3,4,5,7
1504−166	OR−102	15 04 16.4154	−16 40 59.282	0.876	HPQ	2.01	1,2,3,5,7
1510−089	OR−017	15 10 08.9018	−08 54 47.541	0.361	HPQ	2.71	1,2,4,5,6,7
1519−273		15 19 37.2000	−27 19 30.000	>0.2	BLO?	2.26	1,2,3
1548+056	4C05.64	15 48 06.9368	+05 36 11.329	1.422	HPQ	$1.7^\dagger$	1,2,5,6,7
1730−130	NRAO530	17 30 13.5341	−13 02 45.832	0.902	WPQ	$5.2^\dagger$	1,2,4,5,6,7
1741−038	OT−068	17 41 20.6185	−03 48 48.872	1.054	HPQ	2.21	1,2,3,5,6,7
1814−637		18 14 45.9573	−63 47 03.184	0.063	G	$4.21^\ddagger$	1
1921−293	OV−236	19 21 42.2366	−29 20 26.412	0.352	HPQ	14.39	1,2,3,5,7
2134+004	DA553	21 34 05.2126	+00 28 25.023	1.936	WPQ	8.75	1,2,5,6,7
2145+067	4C06.69	21 45 36.0849	+06 43 40.842	0.990	WPQ	5.57	1,2,4,5,6,7
2216−038	4C−3.79	22 16 16.3862	−03 50 40.703	0.901	WPQ	$1.50^\ddagger$	1,2,6,7
2223−052	3C446	22 23 11.0822	−05 12 17.889	1.404	HPQ	$5.4^\ddagger$	1,2,3,4,5,6,7
2345−167	OZ−176	23 45 27.6847	−16 47 52.714	0.576	HPQ	2.11	1,2,3,5,7

Notes to TABLE 1

(1) IAU source name.
(2) Other identification.
(3) Right Ascension (B1950.0).
(4) Declination (B1950.0).
(5) Redshift.
(6) Optical identification (BLO=BL Lac Object; G=Galaxy; HPQ=Highly Polarized Quasar; WPQ=Weakly Polarized Quasar).
(7) Total flux density at 5 GHz in Jy measured at Hartebeesthoek (South Africa), except as noted. These measurements are on the Baars scale (Barrs *et al.* 1977) and the typical errors are about 2%. The values with † were estimated from the unpublished data in the University of Michigan Radio Variability Program at the time of our measurements (Aller & Aller 1995, private communication), while the values with ‡ were taken from the literature.
(8) 1: listed in various Parkes Catalogues (22 of 22), 2: proposed as a target for RadioAstron by the Science Objective Committee (21 of 22), 3: observed and detected at 2.3 GHz by the TDRSS experiment (Linfield *et al.* 1989) (9 of 22), 4: observed and detected at 15 GHz by the TDRSS experiment (Linfield *et al.* 1990) (5 of 22), 5: observed by University of Michigan Radio Astronomy Observatory (UMRAO) at 4.8, 8.0 and 14.5 GHz (Aller and Aller 1995, private communication) (16 of 22), 6: observed at 22 and 37 GHz at Metsähovi Radio Research Station (Valtaoja & Teräsranta 1995, private communication) (13 of 22), 7: observed by the Swedish-ESO Submillimeter Telescope (SEST) at 90 and 230 GHz (Valtaoja & Tornikoski 1995, private communication) (18 of 22).

The post-correlation reduction was carried out at the Harvard-Smithsonian Center for Astrophysics, using the NRAO AIPS and Caltech VLBI analysis packages. We first applied the AIPS global fringe-fitting algorithm. The raw data were edited based on information contained in the log sheets from each station. Then *a priori* amplitude calibrations were applied using the gain curves and system temperatures measured at each station. In the fringe-fitting procedure we used a point-source model and a solution interval of 2.5 minutes. Hobart served as the reference telescope whenever possible. Fringes were found for each source on almost all the baselines.

The AIPS-format data were then converted to the Caltech format for mapping with the program DIFMAP (Shepherd *et al.* 1994) in the Caltech VLBI Package. The 2-second visibility data were coherently time averaged to 60 seconds. The uncertainties in the averaged visibilities were computed from the scatter of data points within the averaging interval. The data were inspected for obviously bad points, most of which were near the start time of a scan when telescopes were still slewing to the sources, and these were removed. The sources were mapped with several iterations of the self-calibration and cleaning procedures. Natural weighting of the data was used for all imaging. A 1-Jy point-source model was employed at the start of each mapping process. On subsequent iterations, the image produced by previous clean cycles was used as an input model for phase corrections. For the amplitude self-calibration, a constant gain factor for each antenna was implemented in the later stage of the mapping. The derived factors for each antenna were usually in good agreement with those obtained by comparing the correlated flux densities on different baselines at the crossing points in the (u,v) plane, where available. Twenty maps were successfully produced for this survey (see Fig. 2 and Table 3).

TABLE 2. Antenna characteristics in 1992 November.

Station Location (Code) (1)		Size (m) (2)	η (%) (3)	T_{sys} (Jy) (4)	Gain (K/Jy) (5)	Pol (6)	Frequency Standard (7)
Hartebeesthoek	(E)	26.0	39	970	0.0740	LCP	H-Maser
Hobart	(Hb)	26.0	52	1400	0.1000	LCP	H-Maser
Mopra	(M)	22.0	61	500	0.0839	LCP	Rubidium
Narrabri	(Cg)	22.0	60	500	0.0830	LCP	Rubidium
Perth	(P)	27.5	48	1400	0.1035	LCP	Rubidium
Seshan	(Sh)	25.0	50	1200	0.0888	LCP	H-Maser

Notes to TABLE 2

(1) Station name and antenna code in parentheses.
(2) Antenna diameter.
(3) Effective antenna aperture efficiency.
(4) System temperature.
(5) System gain factor.
(6) Polarization, IEEE convention.
(7) Type of frequency standard used.

FIG. 1. The typical (u,v) coverage for the SHEVE plus the Shanghai station snapshot observations (1730−130).

We analyzed the images quantitatively using the MODELFIT program in the Caltech VLBI package. Up to three Gaussian components were used to fit both the closure phases and amplitudes in the calibrated data. The results are listed in Table 4. In some cases, the model does not fit the data as precisely as expected based on a χ^2 criterion, indicating that the source distribution is probably more complex than our model. Generally speaking, the models are not unique, and it is possible to find other parameters which yield an acceptable fit to the data. We have generated a family of acceptable models for each source, and found that these do not differ significantly from our adopted models. We have also done Monte Carlo simulation and demonstrated that all the model parameters are robust, with the exception, in some cases, of the component position angle of the major axis. The uncertainties in position angle are large when the signal-to-noise ratio is low (i.e., the component is weak) and/or the axial ratio is close to unity. In all cases we feel that the models given are reasonable representations of the sources.

4. IMAGE AND DISCUSSION OF INDIVIDUAL SOURCES

We discuss the results of each source in our survey in order of right ascension. The maps of the sources are shown in Fig. 2. On each map, the size of the restoring beams is shown as a cross-hatched ellipse in the lower left corner. The lowest contour level in each map is three times the rms noise. The rms noise in the images varied from 5 mJy to 10 mJy per beam for most sources. The values of various parameters for each source (e.g., peak flux density, rms noise, restoring beam, and contour levels) are listed in Table 3. The results of the model-fitting are given in Table 4.

It is useful to make a quantitative determination about whether a source component is resolved (i.e., shows signs of being extended in angle) or unresolved by the interferometer. We established a criterion based on the following analysis. The visibility of a circular Gaussian component is

$$V = V_0 e^{-3.56(\theta_S/\theta_B)^2}, \tag{1}$$
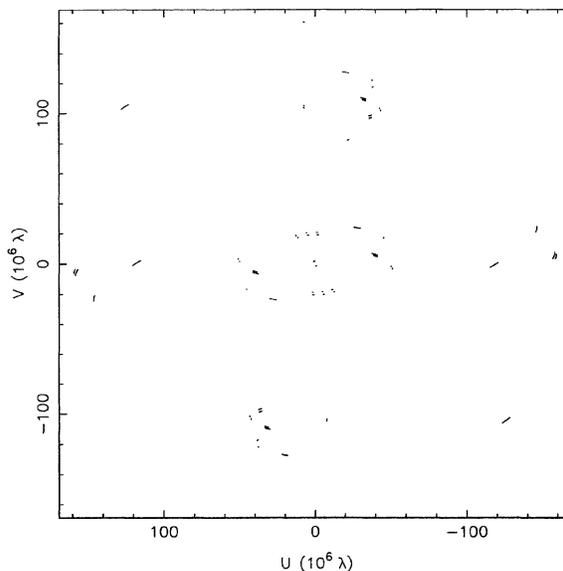
where V_0 is a constant equal to the flux density value for an unresolved source, while θ_B is the resolution (or synthesized beam width) and θ_S is the source size in full width to half maximum intensity (FWHM). It is clear that the source is resolved if $\theta_S > \theta_B$. Therefore, we only consider the case of $\theta_S < \theta_B$. From Eq. (1), we can derive the fractional deviation of visibility as

$$\frac{\Delta V}{V_0} = 3.56 \left(\frac{\theta_S}{\theta_B} \right)^2, \tag{2}$$

where $\Delta V = V_0 - V$ is the decrease in visibility due to resolution. Instrumental contributions to the fractional deviation, $\Delta V/V_0$, might be caused by two terms: a statistical term which is the reciprocal of the signal-to-noise ratio (SNR), and a systematic one, $\Delta F/F$, which is the sum of the uncertainties in the flux density measurements and calibration errors, and is given by

$$\frac{\Delta V}{V_0} = \left[\left(\frac{1}{\text{SNR}} \right)^2 + \left(\frac{\Delta F}{F} \right)^2 \right]^{1/2}. \tag{3}$$

Equating the right-hand sides of Eqs. (2) and (3), we get

$$\theta_{\text{LIM}} = [\theta_{\text{LIM}}(\text{Statistical})^4 + \theta_{\text{LIM}}(\text{Systematic})^4]^{1/4}, \tag{4}$$

where θ_{LIM} is the limit on source size that can be set, and $\theta_{\text{LIM}}(\text{Statistical})$ and $\theta_{\text{LIM}}(\text{Systematic})$ are given by

$$\theta_{\text{LIM}}(\text{Statistical}) = 0.53 \frac{\theta_B}{\sqrt{\text{SNR}}} \tag{5}$$

and

$$\theta_{\text{LIM}}(\text{Systematic}) = 0.53 \frac{\theta_B}{\sqrt{|F/\Delta F|}}. \tag{6}$$
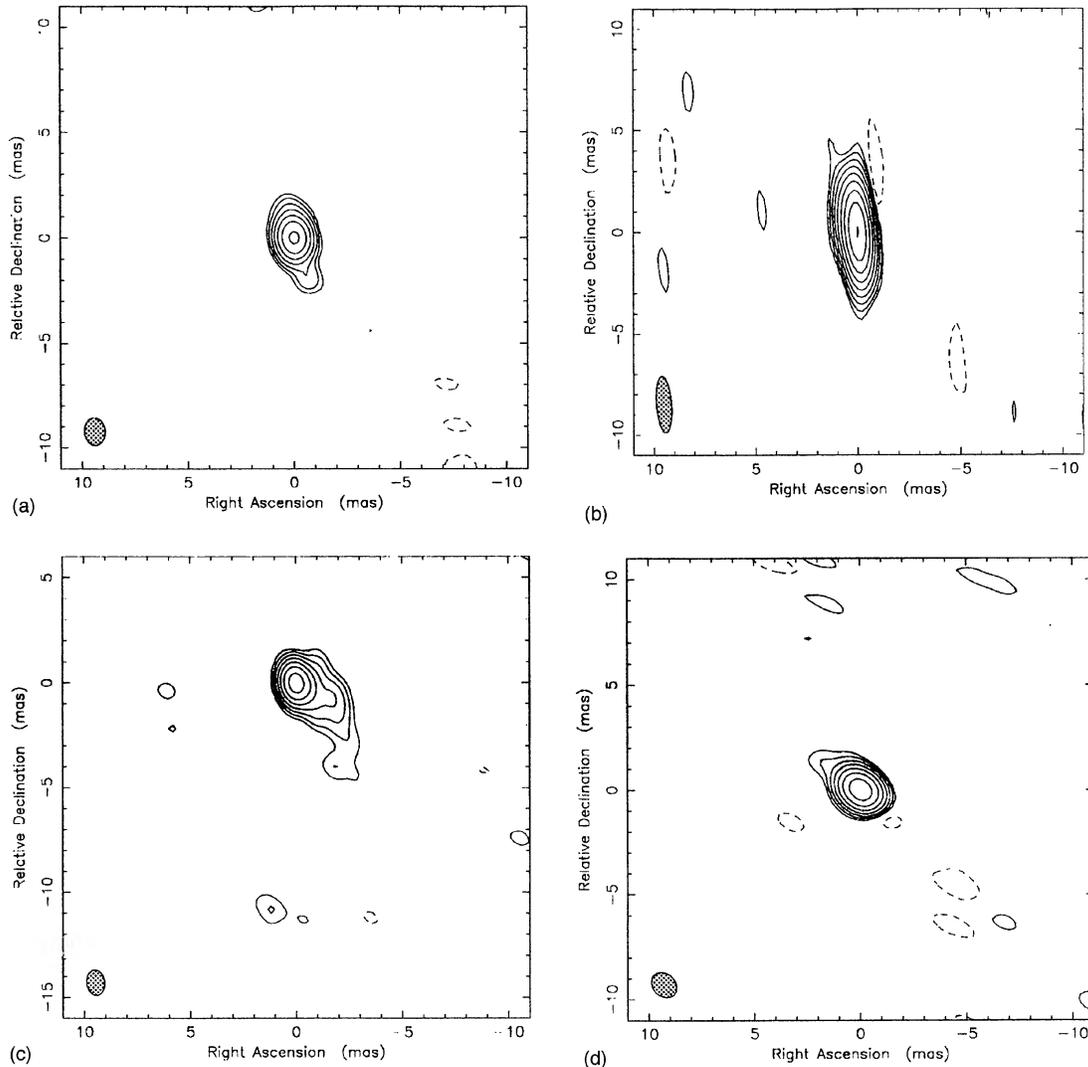
FIG. 2. The VLBI maps of twenty extragalactic radio sources observed in 1989 November. The synthesized beam is shown in the lower left of each map. See Table 3 for detailed parameters.

For our data, $\Delta V/V$ is usually dominated by the systematic errors. If $|\Delta F/F| \sim 0.15$ (a reasonable estimate for our data) and SNR ~ 10, then

$$\theta_{LIM}(\text{Statistical}) = 0.17\theta_B \tag{7}$$

and

$$\theta_{LIM}(\text{Systematic}) = 0.21\theta_B. \tag{8}$$

Since SNR > 10 in all cases in Table 4, θ_{LIM} is always dominated by the systematic term [see Eqs. (4), (7), and (8)], and we adopt

$$\theta_{LIM} = 0.2\theta_B, \tag{9}$$

where we take θ_B to be the geometric mean of the major and minor beam sizes. The results based on this criterion are listed in column 10 of Table 4. Components with fitted sizes smaller than θ_{LIM} in Eq. (9) are listed as unresolved.

The peak brightness temperature of each component in the rest frame of the source is listed in column 9 of Table 4, and was calculated from the relation

$$T_b = 1.22 \times 10^{12} S\nu^{-2} (\theta_{max}\theta_{min})^{-1} (1+z) \quad \text{K,} \tag{10}$$

where S is the flux density in Jy, ν the frequency in GHz (5 GHz in our experiment), z the redshift, and θ_{max} and θ_{min} are the major and minor axes in mas, respectively. For unresolved components, lower limits are provided.

Throughout the paper, we define the spectral index, α, by the convention $S_\nu \propto \nu^\alpha$, and we assume $H_0 = 100$ km s^{-1} Mpc^{-1} and $q_0 = 0.5$. Our search of the literature was greatly assisted by NED.[2]

---

[2]The NASA/IPAC Extragalactic Database (NED) is operated by the Jet Propulsion Laboratory, California Institute of Technology, under contract with the National Aeronautics and Space Administration.

(e)
Right Ascension (mas)

(f)
Right Ascension (mas)

(g)
Right Ascension (mas)

(h)
Right Ascension (mas)
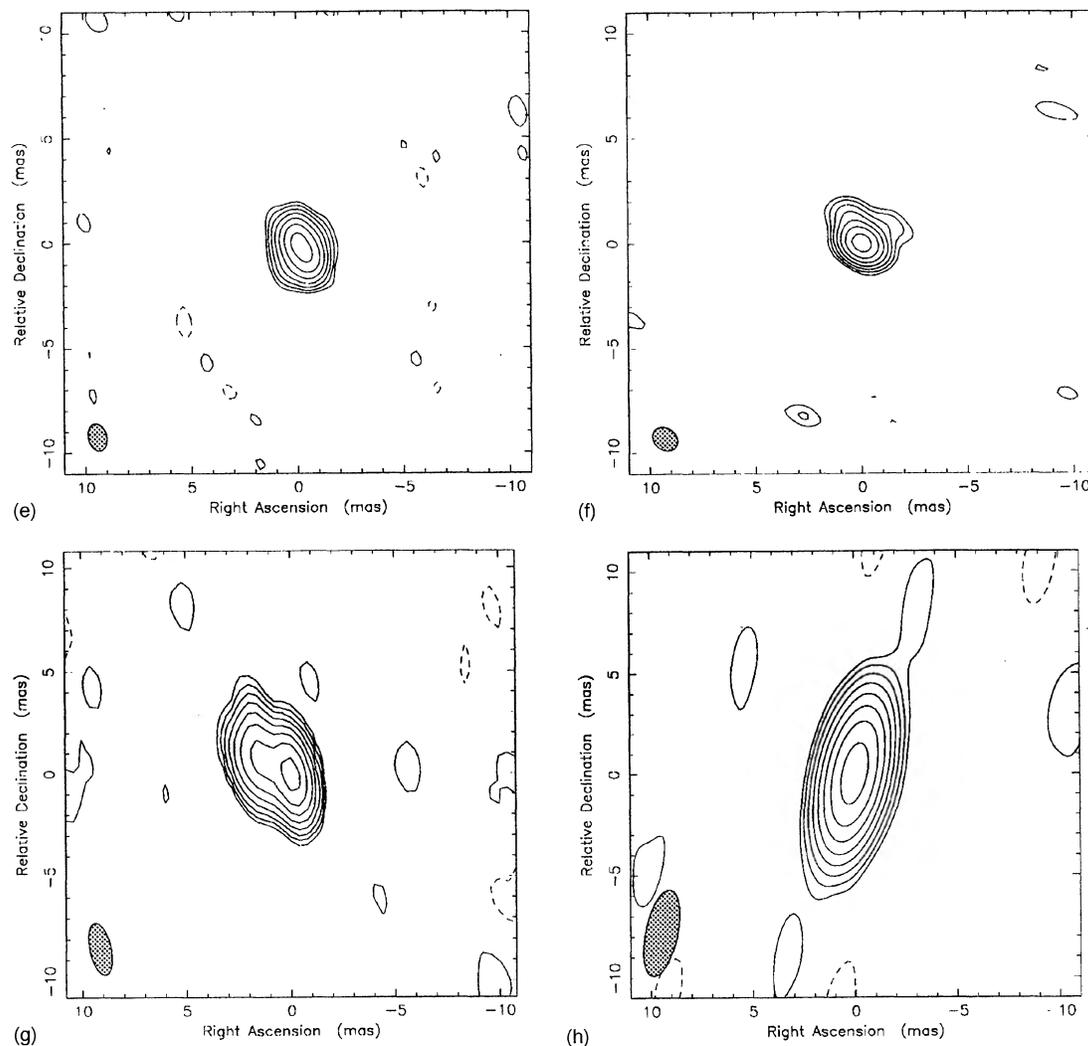
FIG. 2. (continued)

0048−097 [OB−080, Fig. 2(A)]

This is a bright, strongly variable BL Lac object (Andrew & Smith 1983). The absence of the extended nebulosity of the BL Lac host galaxy suggests that $z>0.2$ (Stickel *et al.* 1993). It is highly variable at mm wavelengths (Steppe *et al.* 1988, 1992), which is consistent with its flat spectrum between 8.4 and 90 GHz (Tornikoski *et al.* 1993).

No previous VLBI images have been obtained at any frequency. From earlier VLBI observations at 5 GHz, Weiler & Johnston (1980) estimated the visibility to be 0.89 with total flux density of 0.80 Jy, and Gaussian model diameter of 0.4 mas.

Our observations revealed a core-jet structure extending 2.0 mas from the central core at a position angle (P.A.) of −159°. This orientation is consistent with the large core-jet structure on the scale of 7 arcseconds observed with the VLA (Perley 1982; Wardle *et al.* 1984). The parameters of the compact core (component 1) are in reasonable agreement with the results from Weiler & Johnston (1980) in both visibility and source size, although the flux density has in-

creased about 1.5 times. There is no indication in the radio data of the elongation to the east, which was once seen on an optical CCD image (Falomo *et al.* 1990), but not detected in the subsequent spectroscopic observations (Stickel *et al.* 1993).

0104−408 [Fig. 2(B)]

This 19th magnitude QSO was identified as a possible BL Lac object with a redshift $z=0.584$ (White *et al.* 1988). It is one of the benchmark objects in the establishment of a high-precision radio/optical celestial reference frame (Costa & Loyola 1992). There is no previous radio image of the source.

The source is well-fitted by a single Gaussian component with a flux density of 2.6 Jy and a size of 0.6×0.3 mas at P.A.=19°. It might have a slight extension toward the east. Because of its southern declination, the Shanghai antenna did not contribute to the mapping, which caused a relatively poor synthesized beam (2.8×0.7 mas at P.A.=4°) in the north-south direction. The total flux density was 2.6 Jy, about three
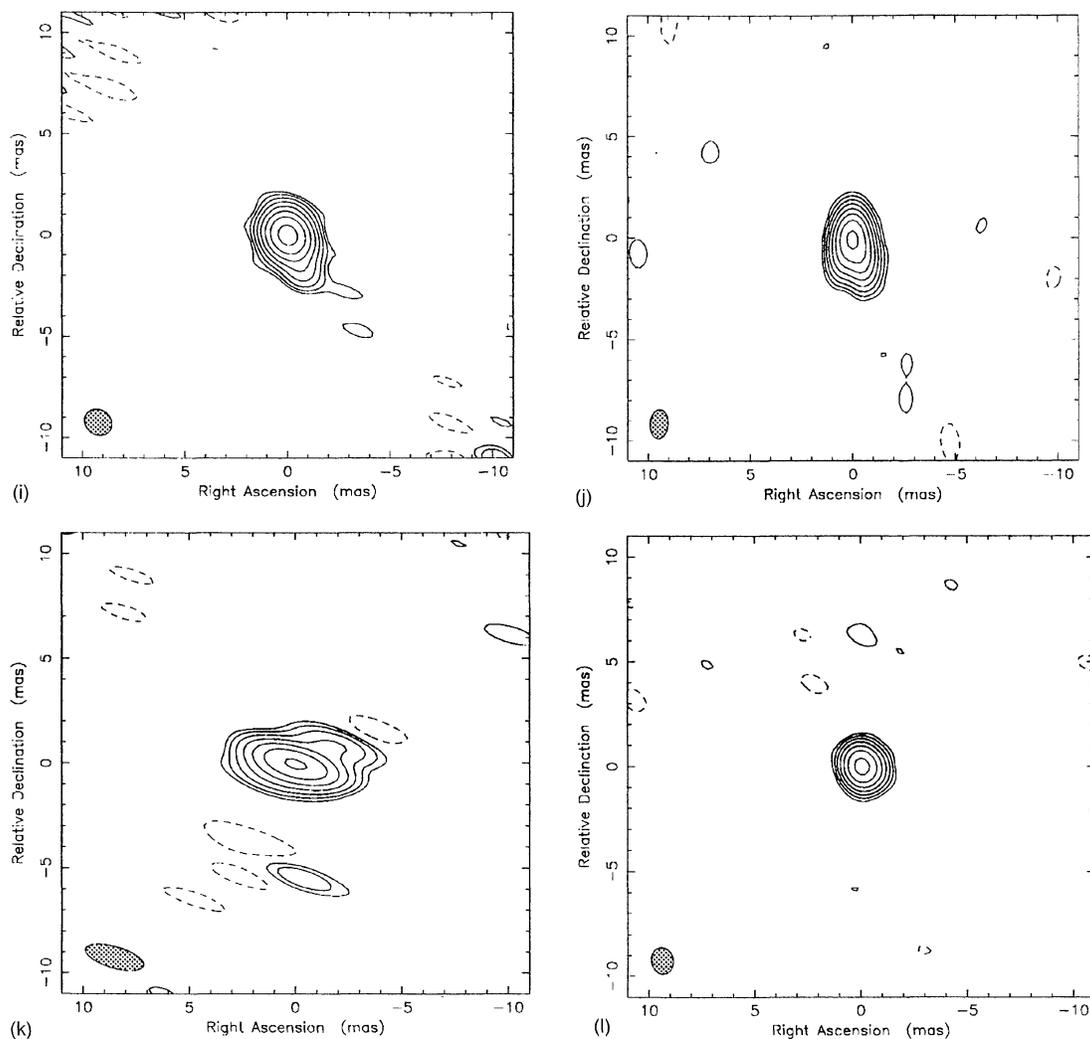
FIG. 2. (continued)

times stronger than at previous epochs (e.g., Quiniento *et al.* 1988). Future observations at higher resolution (such as space VLBI) would be useful to probe the central core.

0106+013 [4C 01.02; OC 012; Fig. 2(C)]

This source is a highly polarized quasar, and with z = 2.107 (Burbidge 1966), has one of the highest redshifts in our sample. Previous two-epoch VLBI observations were made by Wehrle *et al.* (1990b). Their 5-GHz maps showed an east-west structure and a relative component proper motion of $\mu = 0.2$ mas yr^{-1}, corresponding to an apparent superluminal motion with $\beta_{app} = 8.2$. We fit the new data to a model consisting of three Gaussian components. Their parameters are listed in Table 4.

The VLA image at 5 GHz exhibits a weak jet 5 arcseconds long extending to the south (Kollgaard *et al.* 1990). Thus, the jet bends through an angle of 90° moving from the VLBI core to the outer region. Neff & Hutchings (1990) estimated the bending angle to be 85° without detailed justification. Our image, with its good resolution in the north-south direction, clearly shows the curvature in the jet on the mas scale. We note that a high-redshift source is more likely to show a bent jet than a source at low redshift (Barthel & Miley 1988). Higher dynamic-range imaging will help us better define this morphological transition.

Wehrle *et al.* (1990b) could not identify the core because of the lack of spectral index information. Assuming that the relative proper motion is constant (0.2 mas yr^{-1}) along the direction of P.A.$\sim -110°$, we estimate the separation to be 2.03 mas in 1992 November. This is consistent with the distance on our map between components 1 and 3, which are separated by 2.06 mas along a P.A. of $-116°$. However, the flux density of component 3 has decreased dramatically to 0.20 Jy compared with 2.8 Jy in 1986. As for component 1, it was weak in 1986 (0.8 Jy), peaked around 1988 (1.8 Jy), and decreased to 1.5 Jy by 1992. This modest variability suggests that component 1 is most probably the core. A dramatic variation has been observed in the flux density within the region of 1 mas in 1984–1988 (Takahashi & Kurihara 1993). This may be related to a new bright component

Relative Declination (mas)
Right Ascension (mas)
(m)

Relative Declination (mas)
Right Ascension (mas)
(n)

Relative Declination (mas)
Right Ascension (mas)
(o)

Relative Declination (mas)
Right Ascension (mas)
(p)
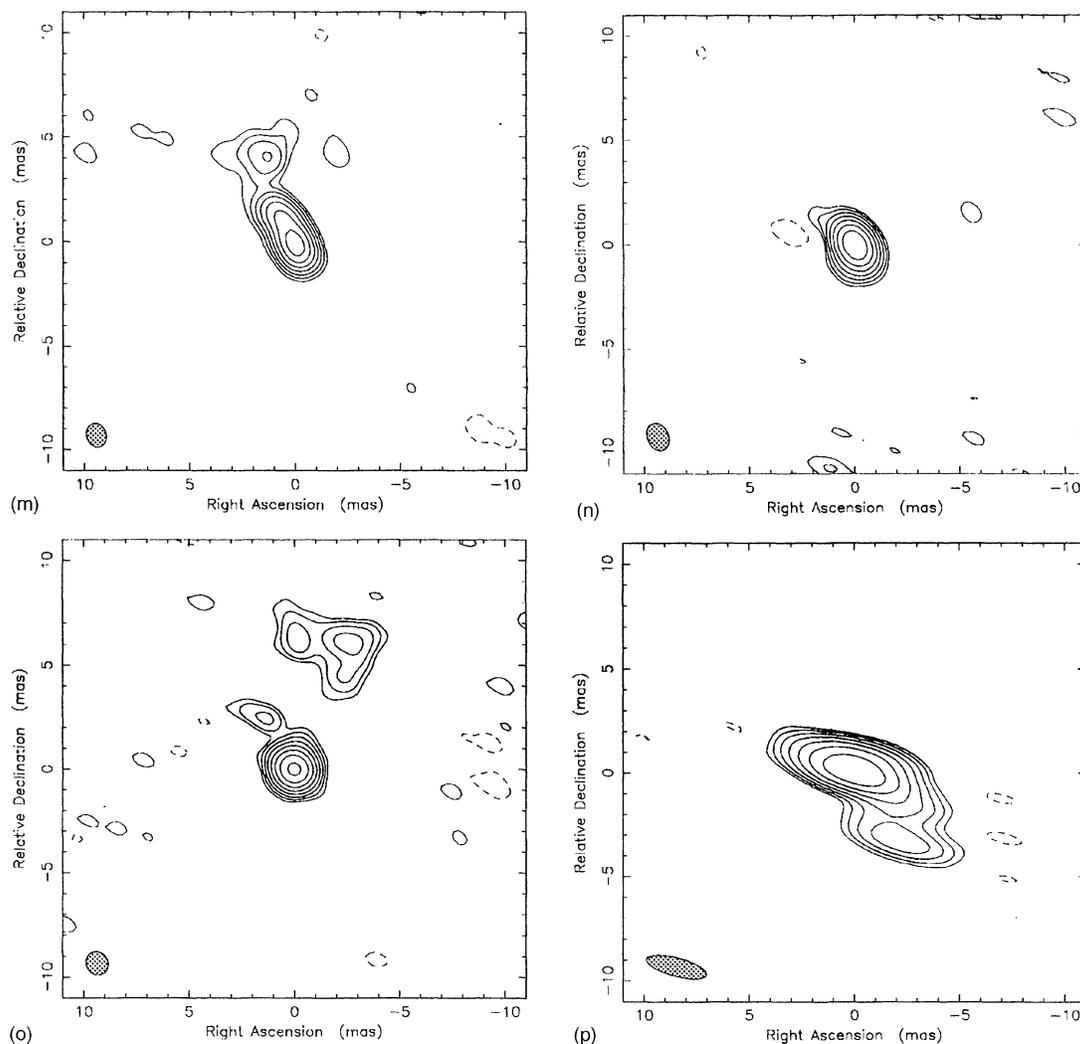
FIG. 2. (continued)

emerging from the core. The peak variation around 1987.8 is probably connected with the emergence of component 2. This implies a proper motion of 0.18 mas yr^{-1}, or a superluminal motion of 7.4c, for component 2.

0235+164 [OD 160; Fig. 2(D)]

This widely studied object is one of the most violently variable sources known (Pollock *et al.* 1979). It is identified with a BL Lac object (Spinrad & Smith 1975), and has three distinct redshifts, one in emission at $z = 0.940$ (Cohen, Smith, & Burbidge 1986), one in absorption at $z = 0.851$ (Burbidge *et al.* 1976), and one in both emission and absorption at $z = 0.524$ (Rieke *et al.* 1976).

In spite of its complex optical features, the radio morphology of 0235+164 is surprisingly simple on both arcsecond and mas scales. The VLA maps at 1.4 GHz and 5 GHz showed no extended emission above 0.1% of the peak flux density of the core (Ulvestad *et al.* 1983; Antonucci & Ulvestad 1985). In the VLBI maps, most of the flux density comes from the central compact core (Jones *et al.* 1984). No

mas polarization structure was found at 5 GHz (Gabuzda *et al.* 1992).

It has been shown that each strong optical and radio outburst is accompanied by the formation of a new VLBI component (e.g., Bååth 1984). These components extend to the northeast, but the position angles vary between 10° and 45° among epochs. Our map, which agrees with such a description, shows a very compact core and a weak shoulder to the northeast (see Table 4). The total flux density measured independently at the time of our experiment at Hartebeesthoek was 4.3 Jy, higher than the typical value ($\sim$3.0 Jy). The brightness temperature of the central core exceeds the Compton limit by a factor of 5 for a redshift of 0.94.

0420−014 [OA 129; Fig. 2(E)]

The 5-GHz image of this flat-spectrum radio quasar exhibits a resolved core (component 1) of 2.0 Jy and a strong secondary component (component 2) of 1.7 Jy along the direction of −146° at a distance of 0.96 mas from the core. The total flux density of 0420−014 obtained from Harte-

(q)   (r)

(s)   (t)
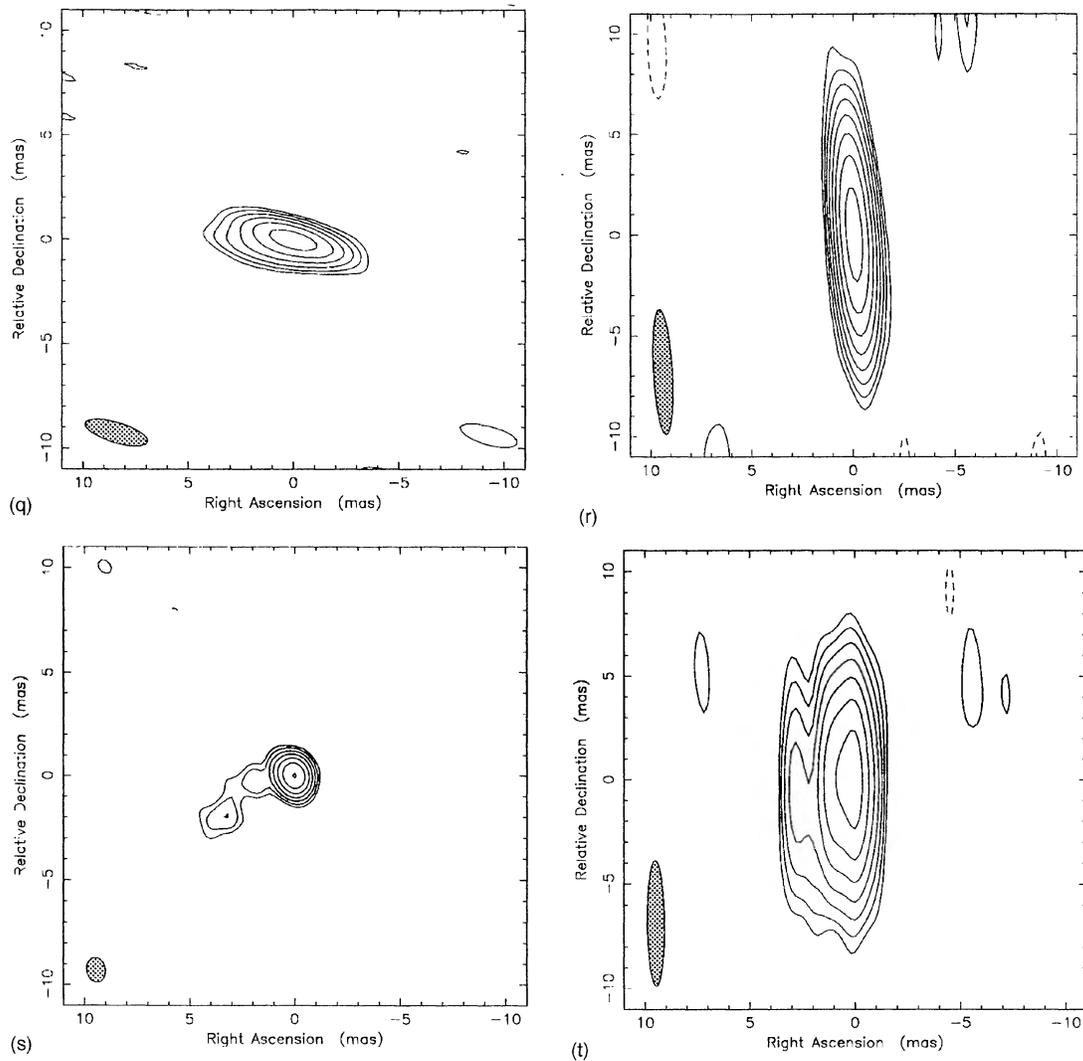
FIG. 2. (continued)

beesthoek is about 4.0 Jy, which is less than that observed by Wehrle *et al.* (1992) in 1986.44. From the radio flux-density curve available (Wehrle *et al.* 1992), the total flux density of 0420−014 reached a peak around 1986.50 at 14.5 GHz, and 1987 at 5.0 GHz. Such a peak may be related to the emergence of a new component, which could explain the tight core-halo structure mapped by Wehrle *et al.*, if the jet lay very close to the line of sight. Assuming that component 2 was ejected at the time of the measurements made by Wehrle *et al.* (i.e., 1986.44), we derive a proper motion of 0.15 mas yr^{-1}, corresponding to an apparent transversal speed of 3.9c at redshift $z=0.915$. This is not surprising if we consider that 0420−014 is one of the γ-ray sources detected by EGRET on the CGRO (von Montigny *et al.* 1995; Radecke *et al.* 1995). Moreover, in the study of geodetic VLBI experiments, Wagner *et al.* (1995) reported a proper motion of 0.15 mas yr^{-1} along a line of P.A.− 142° at the epoch of 1992.15. The jet motion might relate to the southern extended emission revealed by 1.4 GHz VLA observa-

tions (Antonucci & Ulvestad 1985). Further VLBI observations are still needed to confirm these results and study the motion of the jet component.

0458−020 [4C−02.19; Fig. 2(F)]

This source has the highest redshift ($z=2.286$) both in our sample and in the sample of active galactic nuclei detected by EGRET in high-energy γ-rays ($E>100$ MeV) (von Montigny *et al.* 1995). Its radio structure extends over a wide range of scales. The VLA observations at 1.4 GHz (Briggs *et al.* 1989) show two distinct components (1.8 arcseconds in separation with a P.A. of −127°). The VLBI map at 608 MHz (Briggs *et al.* 1989) shows a jet that heads northwest initially and then veers to the southwest. The position angle of the innermost structure is −58°.

Our 5-GHz map confirms the core-jet structure of the source, which was first observed by Wehrle *et al.* (1992). Our map can be represented by three components: a strong

TABLE 3. Source map descriptions.

IAU Name (1)	S_{peak} (Jy/Beam) (2)	rms (Jy/Beam) (3)	Restoring Beam Major (mas) (4)	Restoring Beam Minor (mas) (5)	Restoring Beam P.A. (deg) (6)	Contours (Jy/Beam) (7)	Scale (pc/mas) (8)	VLBI Morphology (9)
0048−097	1.11	0.005	1.3	1.0	4	0.015×(−1,1,2,4,8,16,32,64)	-	core-jet
0104−408	2.35	0.003	2.8	0.7	4	0.009×(−1,1,2,4,8,16,32,64,128,256)	3.8	single core
0106+013	1.42	0.005	1.2	0.9	6	0.015×(−1,1,2,4,8,16,32,64)	4.1	core-jet
0235+164	4.11	0.013	1.3	1.1	44	0.039×(−1,1,2,4,8,16,32,64)	4.2	core-jet
0420−014	1.91	0.007	1.3	0.9	13	0.021×(−1,1,2,4,8,16,32,64)	4.2	core-jet
0458−020	2.49	0.009	1.3	1.0	51	0.027×(−1,1,2,4,8,16,32,64)	4.0	core-jet
1104−445	1.60	0.003	2.6	1.0	13	0.009×(−1,1,2,4,8,16,32,64,128)	4.3	core-jet
1144−379	4.40	0.008	4.3	1.6	−12	0.024×(−1,1,2,4,8,16,32,64,128)	4.3	single core
1334−127	3.70	0.007	1.4	1.2	50	0.021×(−1,1,2,4,8,16,32,64,128)	3.7	core-jet
1504−166	1.37	0.003	1.5	0.9	−4	0.009×(−1,1,2,4,8,16,32,64,128)	4.2	core-jet
1510−089	1.69	0.008	2.9	1.0	73	0.024×(−1,1,2,4,8,16,32,64)	3.1	core-jet
1519−273	2.02	0.008	1.3	1.0	11	0.024×(−1,1,2,4,8,16,32,64)	-	single core
1730−130	2.07	0.007	1.2	0.9	17	0.021×(−1,1,2,4,8,16,32,64)	4.2	core-jet
1741−038	1.88	0.005	1.4	1.0	24	0.015×(−1,1,2,4,8,16,32,64)	4.3	core-jet
1921−293	9.39	0.020	1.2	1.0	28	0.060×(−1,1,2,4,8,16,32,64,128)	3.0	core-jet
2134+004	4.46	0.012	3.0	0.9	75	0.036×(−1,1,2,4,8,16,32,64)	4.1	core-jet
2145+067	4.25	0.030	3.1	1.0	73	0.090×(−1,1,2,4,8,16,32)	4.3	core-jet
2216−038	2.26	0.004	6.2	0.9	3	0.012×(−1,1,2,4,8,16,32,64,128)	4.2	single core
2223−052	3.01	0.015	1.2	0.9	10	0.045×(−1,1,2,4,8,16,32,64)	4.3	core-jet
2345−167	0.88	0.003	6.0	0.8	1	0.009×(−1,1,2,4,8,16,32,64)	3.8	core-jet

Notes to TABLE 3

(1) IAU source name.
(2) Peak flux density.
(3) Rms noise measured in the map.
(4), (5), (6) Parameters of the restoring Gaussian beam: the full width at half maximum (FWHM) of the major and minor axes and the position angle (P.A.) of the major axis.
(7) Contour levels of the map.
(8) Angular size scale (with $H_0 = 100$ km s^{-1} Mpc^{-1} and $q_0 = 0.5$).
(9) Apparent morphology of the source.

compact core (component 1) of 2.6 Jy, and two other resolved weak components (2 and 3). Table 4 describes these components in detail. The detailed description of these components is listed in Table 4. There probably exists a bending angle of ~80° from component 2 to component 3, which then connects to the curvature observed by the VLA (Briggs *et al.* 1989). This will be defined better by higher dynamic range observations.

Comparing the Wehrle *et al.* map (1989.8) with our map, we find that component 3 matches the jet component identified by Wehrle *et al.* Component 2 has no obvious counterpart in the Wehrle *et al.* map, perhaps because of their poorer resolution in the south-north direction. No sign of motion in the jet could be measured. Vermeulen & Cohen (1994) also did not detect proper motion.

1104−445 [Fig. 2(G)]

Partly because of its southern declination, 1104−445 has been less well studied with VLBI, although it is very strong at 5 GHz (3.1 Jy at the time of our experiment). Due to the lack of data for longer baselines to Hartebeesthoek, Preston *et al.* (1989) did not resolve its fine structure at 2.3 GHz with SHEVE in 1982.

The source has a core-jet structure on our map. Its structural parameters are listed in Table 4. There is evidence of jet curvature at a distance of ~1.8 mas moving outward from the core (corresponding to a projected length of ~8.0 pc)

from the northeast to the north. The lack of baselines to the Shanghai antenna caused a relatively poor resolution in the north-south direction (2.6×1.0 mas at P.A.=13° of beam). Further VLBI imaging observations are needed to monitor the changes in the jets.

1144−379 [Fig. 2(H)]

This is a BL Lac object (Nicolson *et al.* 1979) with the highest emission-line redshift ($z = 1.048$) in the 1-Jy sample (Stickel *et al.* 1989, 1991). Considering its high optical variability and polarization, Impey & Tapia (1988) classified it as a blazar. There is no previous VLBI map.

This highly variable radio source was in an active phase at the time of the observations, with a flux density at 5.0 GHz of about 4.6 Jy. Our observations, without baselines to the Shanghai antenna, showed it as unresolved. The visibility data can be fitted by a 0.5 mas×0.4 mas Gaussian component with 4.6 Jy of flux density, which corresponds to a brightness temperature of $2.3×10^{12}$ K. Higher-frequency VLBI observations are important for the investigation of the structural variation of this source.

1334−127 [PKS 1335−127; OP−158.3; Fig. 2(I)]

Based on the optical polarimetry, 1334−127 was classified as a highly polarized quasar, or a blazar (Impey & Tapia 1988, 1990). VLA observations at 1.4 GHz showed a curved jet extending to 6.5 arcseconds east of the core (Perley

TABLE 4. Source model descriptions.

Source IAU Name (1)	Component Number (2)	S (Jy) (3)	r (mas) (4)	θ (deg) (5)	Gaussian Model Major (mas) (6)	Minor (mas) (7)	P.A. (deg) (8)	Brightness Temperature (10^{12} K) (9)	Resolved Structure (10)
0048−097	1	1.22	0.00	0	0.3	0.2	78	1.2	Y
	2	0.10	2.04	−159	2.0	1.8	15	0.002	Y
0104−408	1	2.63	0.00	0	0.6	0.3	19	1.1	Y
0106+013	1	1.48	0.00	0	0.4	0.3	90	1.9	Y
	2	0.34	0.93	−111	0.9	0.9	40	0.06	Y
	3	0.20	2.06	−116	1.5	1.2	44	0.02	Y
0235+164	1	4.45	0.00	0	0.4	0.2	76	5.3	Y
	2	0.12	2.25	58	0.8	0.5	30	0.03	Y
0420−014	1	2.01	0.00	0	0.8	0.6	30	0.4	Y
	2	1.70	0.96	−146	1.1	0.4	141	0.4	Y
0458−020	1	2.62	0.00	0	0.4	0.2	91	5.3	Y
	2	0.26	1.11	19	1.0	0.9	4	0.05	Y
	3	0.15	1.51	−58	4.5	1.9	72	0.003	Y
1104−445	1	1.79	0.00	0	0.5	0.4	90	1.1	Y
	2	0.84	1.66	62	0.8	0.8	0	0.2	Y
	3	0.20	2.68	41	2.0	0.8	6	0.02	Y
1144−379	1	4.64	0.00	0	<0.5	<0.4	87	>2.3	N
1334−127	1	4.10	0.00	0	0.6	0.4	5	1.3	Y
	2	0.60	1.66	−160	0.8	0.2	23	0.3	Y
1504−166	1	1.31	0.00	0	0.5	0.5	0	0.5	Y
	2	0.62	1.12	−156	0.9	0.5	13	0.1	Y
	3	0.34	0.79	161	0.9	0.7	178	0.05	Y
1510−089	1	1.66	0.00	0	<0.3	<0.3	0	>1.2	N
	2	0.34	1.56	−42	<0.2	<0.2	77	>0.6	N
	3	0.12	1.38	107	1.5	0.2	98	0.03	Y
1519−273	1	2.17	0.00	0	<0.4	<0.1	74	>3.2	N
1730−130	1	2.34	0.00	0	0.6	0.3	40	1.2	Y
	2	1.25	1.29	25	1.1	0.6	43	0.2	Y
	3	0.59	3.95	19	1.7	0.8	127	0.04	Y
1741−038	1	2.06	0.00	0	0.6	0.3	57	1.1	Y
	2	0.10	0.84	169	1.0	0.5	130	0.02	Y
1921−293	1	11.12	0.00	0	0.5	0.3	103	4.9	Y
	2	2.17	6.62	−23	2.6	0.8	81	0.07	Y
	3	0.76	3.17	33	1.9	0.5	82	0.05	Y
2134+004	1	6.70	0.00	0	1.0	0.9	1	1.1	Y
	2	1.02	2.49	−122	0.8	0.7	171	0.3	Y
	3	0.94	3.96	−152	1.4	1.1	71	0.09	Y
2145+067	1	4.01	0.00	0	<0.2	<0.2	120	>9.7	N
	2	1.19	1.23	106	0.7	0.6	92	0.3	Y
2216−038	1	2.55	0.00	0	<0.5	<0.5	0	>0.9	N
2223−052	1	3.34	0.00	0	0.5	0.2	87	3.9	Y
	2	0.33	2.27	102	1.8	1.0	130	0.02	Y
	3	0.29	4.18	105	1.9	1.1	154	0.02	Y
2345−167	1	1.57	0.00	0	1.0	0.7	88	0.2	Y
	2	0.30	2.95	116	0.5	0.4	16	0.1	Y

Notes to TABLE 4

(1) IAU source name.
(2) Numerical label; component 1 is taken to be the core.
(3) Flux density of each component.
(4) Distance of each component from the origin defined by component 1.
(5) Position angle of each component with respect to the origin (east of north).
(6), (7), and (8) Parameters of Gaussian model: major and minor axes of each component in mas (FWHM) and the position angle (P.A.) of the major axis.
(9) Peak brightness temperature.
(10) Component is resolved (Y) or unresolved (N) by our experiment [see Eq. (9) for resolution criterion].

1982). Wehrle *et al.* (1992) found, from VLBI observations in 1986.9, that the source was barely resolved.

This source can be represented by a core-jet structure from our observations (see Table 4). The weak jet component is located at 1.7 mas to the core along a direction of −160°, and must bend through about 110° between mas and

arcsecond scales. 1334−127 was at its peak flux density in 1986.9, but was not very active during our observations. It is clear that the source was undergoing an outburst during the observations of Wehrle *et al.* (1992) based on the monitoring observations at 14.5 GHz and 8.4 GHz. Such an outburst would be first detected at higher frequencies and then fol-

lowed at lower frequencies, which could explain the failure of Wehrle *et al.* to detect the jet component at 5 GHz. Assuming the jet component was ejected in 1986.9 with the outburst, we estimate the average transverse angular velocity to be 0.28 mas yr^{-1}, which corresponds to $\beta_{app} = 5.2$ at a redshift of 0.541 (Wilkes 1986). Hence, 1334−127 is a superluminal candidate.

1504−166 [PKS 1504−167; OR−102; Fig. 2(J)]

This source shows low-frequency variability (McAdam 1982; Bondi *et al.* 1994). It is also classified as a highly polarized quasar or blazar (Impey & Tapia 1988, 1990). The 1.7-GHz VLBI two-epoch maps (Romney *et al.* 1984; Padrielli *et al.* 1986) revealed a very compact structure in 1504−166, with a jet component at about 3.5 mas from the compact core towards the direction of 140°.

Our map consists of a circular compact core (component 1) with a flux density of 1.3 Jy and a diameter of 0.5 mas, a 0.6 Jy jet (component 2) at the position angle of −156° and separation of 1.12 mas to the core, and a possible 0.3 Jy component (3) at 0.80 mas to the core with a P.A. of 161°. The third component is close in position angle, but has a different scale-size compared to the jet component at 1.7 GHz (Padrielli *et al.* 1986). All these components are resolved. The difference of about 45° between the position angles of the two components (2 and 3) within 1−2 mas from the core would be interesting for future observations.

1510−089 [OR−017; Fig. 2(K)]

1510−089 has an optical redshift of 0.361 (Burbidge & Kinman 1966), one of the lowest in our sample. It is a core-dominated, highly polarized quasar (Moore & Stockman 1981) with low-frequency variability (Padrielli *et al.* 1987; Ghosh *et al.* 1994). 1510−089 is one of the γ-ray sources detected by EGRET on the CGRO (Thompson *et al.* 1993), and is so compact and strong that fringes have been detected on baselines of 15,000 km by the TDRSS 15-GHz space VLBI (Linfield *et al.* 1990).

Our observations of 1510−089, with an improved north-south resolution, confirmed the asymmetric two-sided structure at 5 GHz (de Waard 1986). Our analysis shows that two of three components (1 and 2) are unresolved (see Table 4). In addition, there is probably weak emission to the south, which may be part of the jet feature extending 4 mas in length in P.A.∼173° observed by Romney *et al.* (1984), and which may also be connected to the arcsecond-scale jet component extending 8 arcseconds at a P.A. of 160° (Perley 1982). The two-sided features, components 2 and 3 on our map, are asymmetric in flux density and in their positions relative to the central component.

Comparing our results with those obtained in 1984.25 at 5 GHz by de Waard (1986), we conclude that the fine structure of the source at 5 GHz has not changed significantly over this eight-year period. The northwest component 3 could be related to the increase in angular size of the compact component at 1.7 GHz in a P.A. of −10° reported by Padrielli *et al.* (1986). The VLA images at 15 and 23 GHz (O'Dea *et al.* 1988) showed a slightly resolved component 300 mas from the core at a position angle of −28°. It is possible that

the northwest component in our map extends from the core initially at a P.A. of −42° and then curves north by ∼15° to point at the 300-mas secondary component. The southeast feature (component 2) could connect to the southern arcsecond structure revealed by many VLA observations (e.g., 1.4 and 5 GHz by Price *et al.* 1993; 5 GHz by Morganti *et al.* 1993) with a bending angle of ∼75°.

1519−273 [Fig. 2(L)]

1519−273 is probably a BL Lac object because of its featureless spectrum (Véron-Cetty & Véron 1993). Its redshift is unknown, but has been assigned a lower limit of 0.2 by Stickel *et al.* (1993). It is highly polarized at optical wavelengths (Impey & Tapia 1988, 1990). It is also one of the GHz-peaked-spectrum radio sources (Gopal-Krishna *et al.* 1983).

The VLA observations at 1.4 and 5 GHz revealed no structure in 1519−273 (Perley 1982). Some sensitive intercontinental one-baseline VLBI surveys (e.g., the 2.3 and 8.4 GHz survey by Morabito *et al.* 1986) suggested that 1519−273 has a very compact core. The source was thought to be the most compact of all the 23 sources detected by the TDRSS 2.3-GHz space VLBI observations (Linfield *et al.* 1989), with a model size of 0.36 mas and an implied brightness temperature of $3.0 \times 10^{12} (1+z)$ K.

Our observations yielded a first VLBI image of 1519−273. From our map, it is unresolved with flux density of 2.2 Jy. Its brightness temperature is greater than 3.2×10^{12} K. We propose that 1519−273 is unresolved and is a candidate calibrator for southern VLBI experiments at 5 GHz.

1548+056 (4C 05.64; No map)

This source is a highly polarized quasar (Impey & Tapia 1990) with a redshift of 1.442 (White *et al.* 1988), and is also classified as a blazar (Impey & Tapia 1988). In the radio band it shows low-frequency variability (Ghosh & Rao 1992). It is a core-dominated quasar with a flat spectrum at radio wavelengths (Ghisellini *et al.* 1993). We could not map 1548+056 due to the very limited data available. The total flux density measured around 1992 was about 1.7 Jy, which is less than the previous value of 3.3 Jy (e.g., Gregory & Condon 1991). The correlated flux density within Australia on baselines less than 3000 km is about 0.5 Jy, while it was not detected on the baselines from Shanghai to Australia. It probably has structure on the scale of about 4 mas.

1730−130 [NRAO 530; Fig. 2(M)]

This source is one of the best-known examples of a highly variable optical extragalactic source with a redshift of 0.902. Its polarizations at both the optical and radio wavelengths, however, are not large and thus 1730−130 is classified as a weakly polarized quasar. As a low-frequency variable radio source, 1730−130 has been extensively monitored (e.g., at 327 MHz by Ghosh *et al.* 1994; at 408 MHz by Bondi *et al.* 1994). With VLBI observations at 10.7 GHz, Marscher & Broderick (1981) modeled 1730−130 as a double circular (0.31 mas in diameter) Gaussian source separated about 1.2 mas along a position angle of −156°, with the flux densities

of northeast and southwest components of 2.0 Jy and 1.6 Jy, respectively.

Romney *et al.* (1984) found that the structure of 1730−130 at 1.6 GHz is oriented in a north-south direction, extending about 26 mas at a P.A.−7°. Based on two-epoch 1.6-GHz VLBI observations, Padrielli *et al.* (1986) suggested that 1730−130 belongs to one of three classes of low-frequency variable sources. Its complex structural variations are not readily interpreted as angular expansion because the separation of components and the component sizes appear unchanged. More likely, a change in the flux density of a single component is responsible for the variation.

We fit our data with a three-component model (see Table 4). It is clear from the map that there is a curvature of the components relative to the central core, from 25° at 1.3 mas (component 2) to 19° at 4.0 mas (component 3). Furthermore, if we accept that these features are connected to the extended northerly emission on the 1.6-GHz maps of Padrielli *et al.*, which has a position angle of −7° at a distance of about 26 mas to the core, then the curvature continues as the jet moves outward.

1741−038 [OT−068; Fig. 2(N)]

This source is a highly polarized quasar (Impey & Tapia 1990) with a redshift of 1.054 (White *et al.* 1988). Some monitoring programs have revealed the presence of flux-density fluctuations at both lower and higher frequencies. The variability at 1.4 and 2.3 GHz was attributed to RISS (Refractive Interstellar Scintillation) (Hjellming & Narayan 1986; Fiedler *et al.* 1987), while the variability at high frequency (15 and 22 GHz) was attributed to the intrinsic change in the source (Hjellming & Narayan 1986). However, the flux density varies much less at 5 GHz. Quirrenbach *et al.* (1992) found intraday variability in 1741−038 with the Bonn 100-m telescope at 5 GHz. They suggested that this scale of variability is preferentially found in those very compact VLBI sources.

Our VLBI image of 1741−038 shows a core-jet structure. The results from model-fitting are listed in Table 4. These are in close agreement with those reported from the study of ESEs (Extreme Scattering Events) in 1741−038 (Fey *et al.* 1995). The brightness temperature of the compact core is about 1.1×10^{12} K, consistent with the measurement of 0.9×10^{12} K from the TDRSS VLBI experiment at 2.3 GHz (Linfield *et al.* 1989).

1814−637 (No map)

This source is the southernmost one in our sample, at $\delta \sim -64°$, beyond the southern limit of the Shanghai antenna. It was identified as a Seyfert 2 galaxy with a redshift of 0.064 (Danziger & Goss 1979; Thompson *et al.* 1990). It has a compact steep spectrum with a spectral index of −0.75 (Kühr *et al.* 1981). We failed to detect fringes on the baselines from Australia to South Africa. Within Australia, 1814−637 had a correlated flux density of ∼1.1 Jy on the shortest baseline of ∼100 km, and approximately 0.4 Jy on the baselines of ∼1300 km. This probably implies a flux density of only ∼1.0 Jy within a central ∼10 mas compo-

nent. No measurement of the total flux density was available during the observations.

1921−293 [OV−236; Fig. 2(O)]

This object is the strongest source in our sample and has the lowest redshift ($z = 0.352$) in the sample of the sources imaged. It is sometimes referred to as a highly polarized quasar (Worrall & Wilkes 1990), sometimes as an optically violent variable quasar (Pica *et al.* 1988), and sometimes as a BL Lac object (Litchfield *et al.* 1994). It may be a blazar (Angel & Stockman 1980), since it exhibits variability at all observed wavelengths.

Because of the southern declination of 1921−293, few mapping observations have been carried out. It was not resolved by the VLA at 5 and 1.4 GHz (de Pater *et al.* 1985; Perley 1982). VLBI experiments at 2.3 GHz (Preston *et al.* 1989) found that it was slightly resolved on baselines within Australia. The TDRSS VLBI experiment at 2.3 GHz (Linfield *et al.* 1989) estimated brightness temperature of $\sim 3.8 \times 10^{12}$ K for its compact core.

Our VLBI map is the first one at 5 GHz. It clearly shows that 1921−293 has a strong compact core (component 1), which contains flux density of 11.1 Jy at 5 GHz, or 77% of the total flux density of about 14.4 Jy, within an area less than one quarter of the beam. The parameters for the other two features are listed in Table 4. This morphology is possibly related to the core activity and jet curvature observed at 7 mm wavelength (Kellermann, private communication). The quality of our data precluded an accurate estimation of the position of component 2. A full-track 5-GHz SHEVE observation in 1993 February showed a jet component along 30°, which is approximately 50° different from what we obtained for component 2. This difference might indicate a precession of the axis of the jet, and is certainly worthy of further investigation.

2134+004 [OX+057; DA 553; PHL 61; Fig. 2(P)]

This source was noted as an optical variable when it was identified with a 17th magnitude stellar object at a redshift of 1.94 (Shimmins *et al.* 1968). It is one of the most luminous objects in the universe. Moore & Stockman (1984) classified it as a weakly polarized quasar. Its radio spectrum peaks at about 5 GHz (Stanghellini *et al.* 1990).

As a core-dominated radio source, 2134+004 is unresolved with the VLA at 5 GHz (Perley 1982). On the parsec scale, it has a complex structure. The earlier VLBI observations of 2134+004 were fit with a collinear triple model at 10.7 GHz (Schilizzi *et al.* 1975) or a two-component model at 5 GHz (Pauliny-Toth *et al.* 1981). From 1987, however, Pauliny-Toth *et al.* (1990) noticed that the fine structure of 2134+004 has shown an increase in its extent, complexity and orientation, without any accompanying radio outburst. It is not clear how the new features are related to those identified in 1970.

Our measurements at 5 GHz show that 2134+004 consists of three resolved components: a strong compact core (component 1) with flux density of 6.7 Jy, and two others (components 2 and 3) separated from component 1 by 2.5 mas at P.A.−122° and by 4.0 mas at P.A.−152°, respec-

tively. Components 2 and 3 both have flux densities of about 1.0 Jy. Component 1 on our map may correspond to the strongest component in the 10.7-GHz map from 1989.27 by Pauliny-Toth *et al.* (1990). The other two components in the 5-GHz map are probably related to the other part of the complex structure at 10.7 GHz. The components appear to become opaque at different frequencies, which makes the comparison of maps obtained at different wavelengths and different epochs difficult. Multi-frequency VLBI monitoring would be extremely useful to identify its core and understand the morphology. It is possible that quasi-stationary shocks similar to those in 3C 454.3 are at work.

2145+067 [4C+06.69; OX+076.1; DA 562; Fig. 2(Q)]

This is a weakly polarized quasar (Wills *et al.* 1992) at a redshift of 0.990. At radio wavelengths it shows low-frequency variability (Mitchell *et al.* 1994). Its spectral distribution peaks at 15 GHz with flux density of 5.4 Jy (Gear *et al.* 1994).

The VLBI observations indicated that 2145+067 is very compact. Linfield *et al.* (1990) detected it on the ground-space baseline (1.38 earth diameters) at 15 GHz and modeled it with a circular Gaussian component of diameter 0.16 mas and flux density of 5.43 Jy. This corresponds to a brightness temperature of 3.3×10^{12} K. With VLBI observations at 5 GHz in 1988.2, Wehrle *et al.* (1992) found a strong, well-resolved component elongated to the southeast, and a diffuse component located at 7.1 mas with P.A. 140°.

The sparse data for 2145+067 restrict the quality of our hybrid mapping. No unique model could be found that fitted the data satisfactorily. A simple model with only two components that fits our data has an unresolved (about 0.2 mas in diameter) strong (4.0 Jy) circular Gaussian component 1, and a secondary (1.2 Jy in flux density) slightly resolved component 2. The 4.0-Jy component probably corresponds to the component detected from space VLBI experiments, considering that 2145+067 is peaked at 15 GHz. Thus its spectral index between 5 GHz and 15 GHz would be 0.3. We assume that the stronger compact component 1 is the core. The secondary compact component 2 is probably related to the diffuse component in the Wehrle *et al.* (1992) maps. If these assignments are correct, a jet curvature must occur, bending ~34° from 1.2 mas to 7.1 mas.

2216−038 [4C−03.79; OY−027; Fig. 2(R)]

A weakly polarized quasar (Impey & Tapia 1990) with a redshift of 0.901, 2216−038 has a complex (or curved) radio spectrum (Kühr *et al.* 1981). It sometimes shows low-frequency variation (Ghosh & Rao 1992). The VLA observations (Perley 1982) found a jet-like feature extending to 8 arcseconds in P.A. 140°, in addition to an unresolved core.

Our visibility data were well-modeled by a single circular Gaussian component, which has a flux density of 2.6 Jy and an angular size of 0.5 mas. Compared to the beam size (6.2×0.9 mas at P.A. 3°), the source is not resolved. This is consistent with the TDRSS 2.3-GHz space VLBI observations of Linfield *et al.* (1989), who estimated its size to be 0.5 mas with a flux density of 1.8 Jy at 2.3 GHz. Therefore,

the compact core has a spectral index of about 0.5 between 2.3 and 5.0 GHz.

2223−052 [3C 446; 4C−05.92; OY−039; NRAO 0687; Fig. 2(S)]

This source is one of the most luminous quasars known and also one of the most rapidly variable. It has the properties of low-frequency variables (Padrielli *et al.* 1987), optically violent variables (Barbieri *et al.* 1990), and highly polarized quasars (Moore & Stockman 1981, 1984). It is sometimes referred to as a BL Lac object (e.g., Miller & French 1978). The redshift of the source is 1.404 (Burbidge *et al.* 1977).

Our map of 2223−052 exhibits a distorted core-jet morphology, which is in good agreement with many previous radio observations. The source has a compact core and possibly two components to the east of the core. Their parameters are given in Table 4. Simon *et al.* (1985) mapped the source at 1.6 GHz with VLBI and found a continuous, slightly curved jet to the east, with a length of ~250 mas. The jet components seen on our map could be the knots consisting of relatively bright emission in this continuous jet. The source was quiescent during our observations, with a measured total flux density of 5.4 Jy at 5 GHz. Our model could account for no more than 75% of single-dish measurement, which implies that a quarter of the emission was resolved.

Based on all the observations available, we suggest the following conclusion about the complex structure of 2223−052. There is a very compact, optically thick core dominating the radio emission at higher frequencies. At 100 GHz, it is less than 30 μas in diameter (Lerner *et al.* 1993). This core is responsible for the extreme activity observed, which makes the determination of its spectral index difficult. Second, there is an asymmetrical jet within the 2 arcsecond region, with some bright knots in it. Beyond this jet there is possible diffuse emission, which was weaker than the 1.3 mJy per 4.4 arcseconds beam detected by Antonucci (1986). The jet is initially ejected from the core at a P.A.−140° at 100−200 μas scale (Lerner *et al.* 1993), bends first clockwise to the north to P.A.~90°−100° at 1−3 mas, and then counterclockwise to the south to P.A. 110° at 4−5 mas (Brown *et al.* 1981; Wehrle *et al.* 1990a; this work). The jet probably continues in a smoothly sinuous curved path toward the east to a distance of ~550−650 mas from the core (Miley *et al.* 1967; Brown *et al.* 1981; Ulvestad *et al.* 1983; Simon *et al.* 1985; Fejes *et al.* 1992), where a sharp bending of ~120° is required in order to align the jet with low-frequency arcsecond emission at P.A.−30° on the 1−2 arcsecond scale (Joshi & Gopal-Krishna 1977; Browne *et al.* 1982). Such a complex three-dimensional structure reminds us that it could be related to the helix in the jet if the axis is very close to the line of sight.

2345−167 [OZ−176; Fig. 2(T)]

This source is a highly polarized quasar (Moore & Stockman 1981) with a redshift of 0.576 (Hewitt & Burbidge 1987). It is an optically violent variable (Webb *et al.* 1988). At radio frequencies, it has a complex spectrum with a peak

around 5 GHz (Kühr *et al.* 1981), and shows low-frequency variation (McAdam & White 1983).

Our map of 2345−167 shows a core-jet structure. The compact core (component 1) is barely resolved with a flux density of 1.6 Jy in an elliptical Gaussian component of 1.0×0.7 mas at a P.A. of 88°, which is in reasonable agreement with the model-fitting results from the TDRSS 2.3-GHz space VLBI (Linfield *et al.* 1989). Considering the estimated flux density of 1.3 Jy at 2.3 GHz from Linfield *et al.* (1989), we derive a spectral index of 0.28 for the core between 2.3 and 5 GHz. The jet (component 2) is also resolved and separated by 3.0 mas from the core at a P.A. of 116° with the flux density of 0.3 Jy. Comparing our map with that from Wehrle *et al.* (1992) at 5 GHz, we note that the strong secondary component in Wehrle *et al.* (1.5 mas from the core at P.A.∼110°) could be the same component as our jet. Thus, we can estimate the proper motion of 0.26 mas yr^{-1}, or an apparent velocity of ∼5.0c.

We suggest the following scenario for the jet's motion. After being ejected from the core, the jet moves out along the direction of ∼110° (Wehrle *et al.* 1992; this work) up to a distance of 5 mas, then turns north to reach a P.A. of 25° at 6 mas (Preston *et al.* 1989), and continues to bend to a P.A. of ∼−5° at 1.8 arcseconds (Perley 1982). It may then bend further clockwise on the scale of 4.0 arcseconds to a P.A. of −130° (Wardle *et al.* 1984).

5. COMPARISON WITH EGRET DETECTION

Fifty-one active galactic nuclei have been detected above 100 MeV by EGRET on board CGRO (Thompson *et al.* 1995). These γ-ray-loud sources are preferentially flat-spectrum, compact, radio-loud sources. Thus, the study of their radio properties is of great importance for our understanding the process of γ-ray emission.

Of our 22 sources, 5 have γ-ray emission detected by EGRET (von Montigny *et al.* 1995). These are 0235+164, 0420−014, 0458−020, 1510−089, and 1741−038. Of these, 1741−038 does not appear in the second EGRET catalog (Thompson *et al.* 1995) because it was detected with statistical significance (3.9) just below the threshold (4.0) for the new catalog. We retain it as a γ-ray source in the discussion. Superluminal motion was detected in one source (β_{app} =3.9c in 0420−014), as discussed in Sec. 4. One (0235 +164) is a BL Lac object, and the remaining four are highly polarized quasars (HPQs). In other words, HPQs are much more easily detected at γ-ray wavelength than any other types. Since HPQs are thought to beam their radio emissions towards observers, we could infer from the close relation between HPQs and γ-ray sources that a kind of similar γ-ray beaming effect is at work, although both emissions could not originate in the same region.

With VLBI maps available for 20 sources, we can obtain their structural parameters and calculate the brightness temperature (T_B), as shown in Table 4. In Fig. 3, we plot the distribution of T_B (or its lower limit) for both the 5 γ-ray sources and the other 15 sources. Figure 3(a) is a histogram of the brightest components in the 20 sources (i.e., those labeled component 1 in Table 4), while Fig. 3(b) includes all
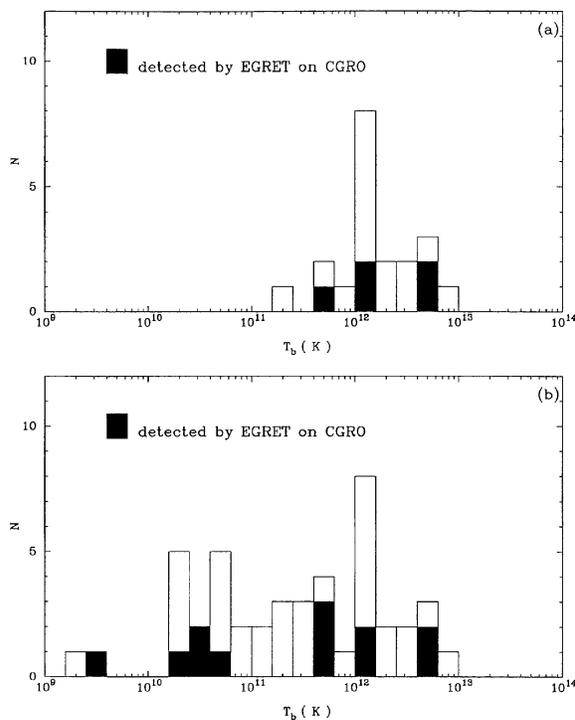
FIG. 3. The histograms of the brightness temperatures, (a) for brightest component in 20 sources mapped and (b) for all 48 components modeled, as shown in Table 4. The black areas correspond to the components in the 5 sources detected at γ-ray wavelength, while the unfilled areas represent those in the other 15 sources.

45 model components in Table 4. The black areas correspond to the components in the sources detected by EGRET, while the unfilled areas represent the others. For those unresolved components, the lower limits of T_B are applied. From Fig. 3(a), the fraction of sources having T_B exceeding 10^{12} K in sources with γ-ray emission detected is 4/5, which is the same as that in the remaining sources (12/15). If we exclude 1741−038 from the γ-ray source list, such a ratio would be 3/4 for sources with γ-ray emission and 13/16 for the others. Comparing Fig. 3(b) with Fig. 3(a), we can see a large range of T_B for the jet-like components, while the distribution of T_B for the strong compact core is around the inverse Compton Limit (∼10^{12} K) with a small spread. The jet components might have less connection to the γ-ray emission. The relativistic beaming effect can be invoked to explain brightness temperatures in excess of the Compton Limit. Therefore, the similarity of T_B distributions in Fig. 3(a), i.e., the fact that more than 75% have T_B greater than 10^{12} K in the subsamples of both γ-ray and non-γ-ray sources, might be an indication of the existence of beamed γ-ray emission too. Furthermore, considering the fact that most γ-ray sources are strongly variable, the similarity and strong correlation of γ-ray sources with radio-loud sources such as HPQs may indicate that all the strong radio variables will be detected in γ-ray emission if they are observed at a suitable time and with small angles to the ejection.

6. SUMMARY

In this paper we have presented southern 5-GHz VLBI observations of compact radio structure in a sample of 22 extragalactic radio sources. The source sample with selection criteria, observations and data reduction were described. Most of these sources show strong variability at the radio wavelengths. This is the first VLBI imaging survey carried out at 5 GHz for equatorial and southern radio sources. Our work redresses the absence of information at frequencies between 2.3 GHz and 8.3 GHz.

Generally, the quality of the maps depends on the (u,v) coverage, sensitivity, and uncertainties in the calibration. Our examples show that we could obtain the basic information for most sources even with snapshot-mode observations. Although we were forced by the limited data to favor the simplest models, we believe that most sources in our sample were well represented by them.

The main conclusions drawn in this paper are:

(1) We have detected fringes from all 22 sources on almost all the baselines. We mapped 20 of the 22 sources detected. Of these 22 sources, six (0048−097, 0104−408, 1144−379, 1519−273, 1741−038, and 2216−038) have never been mapped before. Fifteen of the sources show a core-jet structure, one (1510−089) may have a two-sided jet and four (0104−408, 1144−379, 1519−273, and 2216−038) have a single compact component. There is no compact double, which is consistent with the fact that few compact double sources show variability. The new information for these southern sources will be helpful in determining targets for future space VLBI missions.

(2) The curvature of the jet (i.e., the significant change in the position angle of jet components) from mas to arcsecond scale, sometimes between a few mas to 10 or 100 mas scale, seems to be a common feature. We found eleven examples (0106+013, 0458−020, 1104−445, 1334−127, 1510−089, 1730−130, 1921−293, 2134+004, 2145+067, 2223−052, and 2345−167) in the total of sixteen core-jet sources.

(3) We compared our maps to previous ones and estimated the ejection time from peaks in the flux-density curves at radio wavelengths. We confirmed the superluminal speed

of 8.2c for one component, and suggested a new superluminal motion of 7.4c for another component in 0106+013. The superluminal motions were inferred for three other sources (3.9c in 0420−014, 5.2c in 1334−127, and 5.0c in 2345−167). These values are typical of superluminal speeds in the strong, variable quasars. The results need to be confirmed by future VLBI observations.

(4) Further VLBI observations of southern radio sources would be important not only for expanding the source sample, but for confirming the observed structures (such as bending and superluminal motion) and providing multi-epoch observations, which are necessary for the study of variability.

(5) There are five sources (0235+164, 0420−014, 0458−020, 1510−089, and 1741−038) having γ-ray emissions detected by EGRET (von Montigny *et al.* 1995). Analysis reveals the dominance of highly polarized quasars among the γ-ray sources. Comparison of VLBI measurements with EGRET detection shows a similarity of T_B distribution between these γ-ray sources and others. Taken together, these imply the existence of the beamed γ-ray emission.

REFERENCES

Andrew, J. P., & Smith, A. G. 1983, ApJ, 272, 11
Angel, J. R. P., & Stockman, H. S. 1980, ARA&A, 18, 321
Antonucci, R. R. J., & Ulvestad, J. S. 1985, ApJ, 294, 158
Antonucci, R. R. J. 1986, ApJ, 304, 634
Bååth, L. B. 1984, in VLBI and Compact Radio Sources, IAU Symposium No. 110, edited by R. Fanti, K. I. Kellermann, and G. Setti (Reidel, Dordrecht), p. 127
Barbieri, C., Vio, R., Cappellaro, E., & Turatto, M. 1990, ApJ, 359, 63
Barthel, P. D., & Miley, G. 1988, Nature, 333, 319
Bondi, M., Padrielli, L., Gregorini, L., Mantovani, F., Shapirovskaya, N., & Spangler, S. R. 1994, A&A, 287, 390
Briggs, F. H., Wolfe, A. M., Liszt, H. S., Davis, M. M., & Turner, K. L. 1989, ApJ, 341, 650
Brown, R. L., Johnston, K. J., Briggs, F. H., Wolfe, A. M., Neff, S. G., & Walker, R. C. 1981, Astrophysics Lett., 21, 105
Browne, I. W. A., *et al.*, 1982, Nature, 299, 788
Burbidge, E. M. 1966, ApJ, 143, 612

Burbidge, E. M., & Kinman, T. D. 1966, ApJ, 145, 654
Burbidge, E. M., Caldwell, R. D., Smith, H. E., Liebert, J., & Spinrad, H. 1976, ApJL, 205, L117
Burbidge, G. R., Crowne, A. H., & Smith, H. E. 1977, ApJS, 33, 113
Cohen, R. D., Smith, H. E., & Burbidge, E. M. 1986, BAAS, 18, 674
Costa, E., & Loyola, P. 1992, A&AS, 96, 183
Danziger, I. J., & Goss, W. M. 1979, MNRAS, 186, 93
de Pater, I., Schloerb, F. P., & Johnson, A. H. 1985, AJ, 90, 846
de Waard, G. J. 1986, Thermal-Nonthermal Relationships in Active Galactic Nuclei (Sterrewacht, Leiden), p. 73
Falomo, R., Melnick, J., & Tanzi, E. G. 1990, Nature, 345, 692
Fejes, I., Porcas, R. W., & Akujor, C. E. 1992, A&A, 257, 459
Fey, A., Clegg, A., & Fiedler, R. 1995, BAAS, 27, 863
Fiedler, R. L., *et al.* 1987, ApJS, 65, 319
Gabuzda, D. C., Cawthorne, T. V., Roberts, D. H., & Wardle, J. F. C. 1992, ApJ, 388, 40
Gear, W. K., *et al.* 1994, MNRAS, 267, 167

Ghisellini, G., Padovani, P., Celotti, A., & Maraschi, L. 1993, ApJ, 407, 65

Ghosh, T., & Rao, A. P. 1992, A&A, 264, 203

Ghosh, T., Gopal-Krishna, & Rao, A. P. 1994, A&AS, 106, 29

Gopal-Krishna, Patnaik, A. R., & Steppe, H. 1983, A&A, 123, 107

Gregory, P. C., & Condon, J. J. 1991, ApJS, 75, 1011

Henstock, D. R., et al. 1995, ApJS, 100, 1

Hewitt, A., & Burbidge, G. 1987, ApJS, 63, 1

Hirosawa, H. 1991, in Frontiers of VLBI, edited by H. Hirabayashi, M. Inoue, and H. Kobayashi (Universal Academy Press, Tokyo), p. 21

Hjellming, R. M., & Narayan, R. 1986, ApJ, 310, 768

Impey, C. D., & Tapia, S. 1988, ApJ, 333, 666

Impey, C. D., & Tapia, S. 1990, ApJ, 354, 124

Jauncey, D. L., et al. 1989, AJ, 98, 44

Jauncey, D. L., et al. 1994, in Very High Resolution Imaging, IAU Symposium No. 158, edited by J. G. Roberston and W. J. Tango (Kluwer, Dordrecht), p. 131

Jones, D. L., Bååth, L. B., Davis, M. M., & Unwin, S. C. 1984, ApJ, 284, 60

Joshi, M. N., & Gopal-Krishna 1977, MNRAS, 178, 717

Kardashev, N. S., & Slysh, V. I. 1988, in The Impact of VLBI on Astrophysics and Geophysics, IAU Symposium No. 129, edited by M. J. Reid and J. M. Moran (Kluwer, Dordrecht), p. 433

Kollgaard, R. I., Wardle, J. F. C., & Roberts, D. H. 1990, AJ, 100, 1057

Kühr, H., Witzel, A., Pauliny-Toth, I. I. K., & Nauber, U. 1981, A&AS, 45, 367

Lerner, M. S., et al. 1993, A&A, 280, 117

Linfield, R. P., et al. 1989, ApJ, 336, 1105

Linfield, R. P., et al. 1990, ApJ, 358, 350

Litchfield, S. J., Robson, E. J., & Stevens, J. A. 1994, MNRAS, 270, 341

Marscher, A. P., & Broderick, J. J. 1981, ApJ, 249, 406

McAdam, W. B. 1982, in Proc. Workshop on Low Frequency Variability of Extragalactic Radio Sources, edited by W. D. Cotton and S. R. Spangler (NRAO, Green Bank), p. 141

Meier, D. L., et al. 1989, AJ, 98, 27

Miley, G. K., Rickett, B. J., & Gent, H. 1967, Nature, 216, 974

Miller, J. S., & French, H. B. 1978, in Pittsburgh Conference On BL Lac Objects, edited by A. M. Wolfe (Department of Physics and Astronomy, University of Pittsburgh), p. 228

Mitchell, K. J., et al. 1994, ApJS, 93, 441

Moore, R. L., & Stockman, H. S. 1981, ApJ, 243, 60

Moore, R. L., & Stockman, H. S. 1984, ApJ, 279, 465

Morabito, D. D., Niell, A. E., Preston, R. A., Linfield, R. P., Wehrle, A. E., & Faulkner, J. 1986, AJ, 91, 1038

Morganti, R., Killeen, N. E. B., & Tadhunter, C. N. 1993, MNRAS, 263, 1023

Neff, S. G., & Hutchings, J. B. 1990, AJ, 100, 1441

Nicolson, G. D., Glass, I. S., Feast, M. W., & Andrews, P. J. 1979, MNRAS, 189, 29p

O'Dea, C. P., Barvainis, R., & Challis, P. M. 1988, AJ, 96, 435

Padrielli, L., et al. 1986, A&A, 165, 53

Padrielli, L., et al. 1987, A&AS, 67, 63

Pauliny-Toth, I. I. K., Preuss, E., Witzel, A., Graham, D., Kellermann, K. I., & Rönnäng, B. 1981, AJ, 86, 371

Pauliny-Toth, I. I. K., Zensus, A., Cohen, M. H., Alberdi, A., & Shaal, R. 1990, in Parsec-Scale Radio Jets, edited by J. A. Zensus and T. J. Pearson (Cambridge University Press, Cambridge), p. 55

Pearson, T. J., & Readhead, A. C. S. 1981, ApJ, 248, 61

Pearson, T. J., & Readhead, A. C. S. 1988, ApJ, 328, 114

Perley, R. A. 1982, AJ, 87, 859

Pica, A. J., Smith, A. G., Webb, J. R., Leacock, R. J., Clements, S., & Gombola, P. P. 1988, AJ, 96, 1215

Polatidis, A. G., et al. 1995, ApJS, 98, 1

Pollock, J. T., Pica, A. J., Smith, A. G., Leacock, R. J., Edwards, P. L., & Scott, R. L. 1979, AJ, 84, 1658

Preston, R. A., Morabito, D. D., Williams, J. G., Faulkner, J., Jauncey, D. L., & Nicolson, G. D 1985, AJ, 90, 1599

Preston, R. A., et al. 1989, AJ, 98, 1

Price, R., Gower, A. C., Hutchings, J. B., Talon, S., Duncan, D., & Ross, G. 1993, ApJS, 86, 365

Quiniento, Z. M., Cersosimo, J. C., & Colomb, F. R. 1988, A&AS, 76, 21

Quirrenbach, A., et al. 1992, A&A, 258, 279

Radecke, H.-D., et al. 1995, ApJ, 438, 659

Rieke, G. H., Grasdalen, G. L., Kinman, T. D., Hintzen, P., Wills, B. J., & Wills, D. 1976, Nature, 260, 754

Romney, J., et al. 1984, A&A, 135, 289

Schilizzi, R. T., et al. 1975, ApJ, 201, 263

Shepherd, M. C., Pearson, T. J., & Taylor, G. B. 1994, BAAS, 26, 987

Shimmins, A. J., Searle, L., Andrew, B. H., & Brandie, G. W. 1968, Astrophysics Lett., 1, 167

Simon, R. S., Johnston, K. J., & Spencer, J. H. 1985, ApJ, 290, 66

Spinrad, H., & Smith, H. E. 1975, ApJ, 201, 275

Stanghellini, C., O'Dea, C. P., Baum, S. A., & Fanti, R. 1990, in Compact Steep-Spectrum and GHz-Peaked Spectrum Radio Sources, edited by C. Fanti, R. Fanti, C. P. O'Dea, and R. T. Schilizzi (Instituto di Radioastronomia, Bologna), p. 55

Steppe, H., H., Salter, C. J., Chini, R., Kreysa, E., Brunswig, W., & Pérez, J. L. 1988, A&AS, 75, 317

Steppe, H., Liechti, S., Mauersberger, R., Kömpe, C., Brunswig, W., & Ruiz-Moreno, M. 1992, A&AS, 96, 441

Stickel, M., Fried, J. W., & Kühr, H. 1989, A&AS, 80, 103

Stickel, M., Padovani, P., Urry, C. M., Fried, J. W., & Kühr, H. 1991, ApJ, 374, 431

Stickel, M., Fried, J. W., & Kühr, H. 1993, A&AS, 98, 393

Takahashi, Y., & Kurihara, N. 1993, PASJ, 45, 497

Taylor, G. B., et al. 1994, ApJS, 95, 345

Thakkar, D. D., et al. 1995, ApJS, 98, 33

Thompson, D. J., Djorgovski, S., & De Carvalho, R. 1990, PASP, 102, 1235

Thompson, D. J., et al. 1993, ApJ, 415, L13

Thompson, D. J., et al. 1995, ApJS, 101, 259

Tornikoski, M., Valtaoja, E., Teräsranta, H., Lainela, M., Bramwell, D., & Botti, L. C. L. 1993, AJ, 105, 1680

Tzioumis, A. K., et al. 1989, AJ, 98, 36

Ulvestad, J. S., Johnston, K. J., & Weiler, K. W. 1983, ApJ, 266, 18

Vermeulen, R. C., & Cohen, M. H. 1994, ApJ, 430, 467

Véron-Cetty, M.-P., & Véron, P. 1993, A&AS, 100, 521

von Montigny, C., et al. 1995, ApJ, 440, 525

Wagner, S. J., et al. 1995, A&A, 298, 688

Wardle, J. F. C., Moore, R. L., & Angel, J. R. P. 1984, ApJ, 279, 93

Webb, J. R., Smith, A. G., Leacock, R. J., Fitzgibbons, G. L., Gombola, P. P., & Shepherd, D. W. 1988, AJ, 95, 374

Wehrle, A. E., Cohen, M. H., & Unwin, S. C. 1990a, in Parsec-Scale Radio Jets, edited by J. A. Zensus and T. J. Pearson (Cambridge University Press, Cambridge), p. 49

Wehrle, A. E., Cohen, M. H., & Unwin, S. C. 1990b, ApJ, 351, L1

Wehrle, A. E., Cohen, M. H., Unwin, S. C., Aller, H. D., Aller, M. F., & Nicolson, G. 1992, ApJ, 391, 589

Weiler, K. W., & Johnston, K. J. 1980, MNRAS, 190, 269

White, G. L., et al. 1988, ApJ, 327, 561

Wilkes, B. J. 1986, MNRAS, 218, 331

Wills, B. J., Wills, D., Breger, M., Antonucci, R. R. J., & Barvainis, R. 1992, ApJ, 398, 454

Worrall, D. M., & Wilkes, B. J. 1990, ApJ, 360, 396

Xu, W., Readhead, A. C. S., Pearson, T. J., Polatidis, A. G., & Wilkinson, P. N. 1995, ApJS, 99, 297